KERNFORSCHUNGSZENTRUM

KARLSRUHE

Juni 1974

KFK 1990
EUR 4975 e

Institut für Angewandte Systemtechnik und Reaktorphysik
Projekt Schneller Brüter

Calculation of the Effects of Fission Gas in a LMFBR, for the Analysis of an Unprotected Overpower Transient

H.G. Bogensberger

C. Ronchi (Europaeisches Institut für Transurane)

GESELLSCHAFT
FÜR
KERNFORSCHUNG M.B.H.

KARLSRUHE

GESELLSCHAFT FÜR KERNFORSCHUNG M. B. H.
KARLSRUHE

KERNFORSCHUNGSZENTRUM KARLSRUHE

1974

KFK 1990
EUR 4975e

Projekt Schneller Brüter

Calculation of the Effects of Fission Gas in an LMFBR, for the Analysis of an Unprotected Overpower Transient

H.G. Bogensberger
Institut für Angewandte Systemtechnik
und Reaktorphysik

C. Ronchi
Europaeisches Institut für Transurane
EURATOM

Gesellschaft für Kernforschung mbH., Karlsruhe

Calculation of the Effects of Fission Gas in an LMFBR, for the Analysis of an Unprotected Overpower Transient

Abstract

A distribution model for the noble gases, created by fission, is applied in a computer program. The subroutine LANGZEIT calculates the "long time" behaviour of the fission gas in a pin during "steady state" operation. The results of this calculation are used as the initial conditions for the subroutine KURZZEIT. This code permits the calculation of migration phenomena and pin swelling during an overpower transient. The results for 2 examples are shown and discussed.

31.5.1974

Untersuchungen über den Einfluß von Spaltgasen in schnellen Leistungsreaktoren zur Analyse von Leistungstransienten

Zusammenfassung

Ein Verteilungsmodell für die bei Kernspaltung erzeugten Edelgase wird in einem Computer-Programm durchgerechnet. Die Subroutine LANGZEIT berechnet die Verteilung der Gase in einem Brennstab während des stationären Reaktorbetriebes. Diese berechneten Konzentrationen dienen dann in der Subroutine KURZZEIT als Anfangsbedingungen. In KURZZEIT werden dann Diffusionsphänomene und Brennstoffschwellen während einer Leistungstransiente berechnet. Die Ergebnisse für 2 Reaktoren werden diskutiert.

Table of Contents

1. Introduction

During the last years a great amount of effort has been involved in the development of code systems, such as SAS-VENUS, which permit the analysis of a hypothetical LMFBR accident. These accidents are initiated with a postulated reactivity ramp or a pump failure. As a further hypothetical assumption a complete failure of the shut-down system is requested. Then, sodium voiding or fuel slumping causes a fast reactivity ramp which leads to a prompt critical nuclear excursion. The evaporation of fuel and the outward movement of core material due to the associated pressure gradient, represents the shut-down mechanism which ultimately terminates such an excursion. Heusener and Kessler /1/ and Bohl /2/ made a calculation for the SNR-300 by using the ANL SAS-VENUS-code system. The ANL equation of state, however, treats the fuel as pure UO_2 and neglects the fission gases. Therefore the analysis predicted a substantial energy release in such an excursion and a rather large amount of molten fuel present in the core after the shut-down.

Bogensberger and Fischer /3/ however, have shown that the energy release and the mass of molten fuel, in the same type of accident, will be substantially reduced by taking into account the noble gases enclosed in the fuel.

Therefore it seems to be rather important to develop a theoretical model /4/ which describes the fission gas behaviour in the fuel as a function of the irradiation time and operating temperature. This distribution can be used as the initial conditions for a disassembly analysis. But this "steady state" distribution will be changed by the fast temperature increase during a super prompt transient. In this work the attempt is made to calculate not only the "steady state" gas distribution as a function of space, irradiation time, and operating temperature but also to study the short-time migration phenomena during a transient.

2. Method of analysis of in-pile fission gas behaviour

2.1 Basic assumptions

The gas created by fission during the time life of a core in an LMFBR is subjected to complex kinetic processes. As the thermodynamic solubility of rare gase in nuclear fuels is very low, the main tendency of the gas is to form bubbles or to precipitate into pre-existent void spaces (e.g. sintering porosity).

On the other hand the continuous bombardement of the fission gas bubbles by fission fragments leads to collision events which result in a rejection of gas atoms into the lattice. Therefore the behaviour of the fission gas is mainly determined by these three concomitant effects. In order to describe mathematically the kinetics of fission gas it is useful to define their corresponding rates namely:

db ... rate of precipitation of gas into bubbles

dR ... rate of fission fragment re-injection of gas from bubbles

dg ... rate of precipitation of gas into voids or other stable sinks.

The balance of the three effects leads to the following differential equation:

$$dc = \beta dt - db + dR - dg \qquad (1)$$

where β is the gas production rate and c is the concentration of gas in solution. The integration of equation (1) leads to relationship

$$\beta \cdot t = c + b + g \tag{2}$$

which corresponds to the total balance of the created gas $\beta \cdot t$, distributed in the different phases c (soluted), b (in bubbles) and g (in sinks).

2.2 Deduction of the analytical form of equation (1)

As a first step one needs a correlation of the distribution of gas filled bubbles with the concentration of gas atoms in solution. For this purpose we assume a homogeneous distribution of the bubbles.

Inside of a volume element δV, which is the Wigner-Seitz cell associated with one bubble, one has the diffusion equation

$$\dot{c} = D \Delta c \tag{3}$$

During the diffusion process, the spatial equilibrium is approached quickly, and the time dependence of the equilibrium distribution is given by

$$c = c_o \exp(-t/\tau)$$

with (4)

$$\tau = (4\Pi\, n\, r_o\, D)^{-1}$$

where n is the concentration of bubbles per cm^3, D the diffusion coefficient and r_o the radius of the bubble.

The derivative is

$$\dot{c} = \frac{-c}{\tau} \quad (5)$$

Equation (5) gives the concentration of gas in solid material for a uniform distribution of bubbles. But under operational conditions the case is more complicated. One has to take into account

- gas is produced continuously with the rate β
- fission events cause a certain resolution
- a certain amount of gas precipitates at grain boundaries where it may behave differently from gas in an intragranular bubble.

The resolution rate of gas can be calculated with the model of Nelson /10/

$$\Gamma = \frac{4\Pi\, r_o^2\, d \cdot \eta}{b} \quad (6)$$

Γ resolution rate for the gas in one bubble, mole/sec

b Van der Waals covolume, cm^3/mole

η escape probability, sec^{-1}

d shell thickness of bubble, cm

Under the assumption that growth of bubble does not create strains around the surface, the concentration (in moles) of gas in a bubble is given by

$$m = \frac{8\Pi \, \sigma \, r_o^2}{3 \, R \, T}$$

σ surface tension

with a concentration n of bubbles per cm^3 and homogeneous growth one obtains

$$\frac{\beta t - c^+}{n} = \frac{8\Pi \, \sigma \, r_o^2}{3 \, R \, T} \qquad (7)$$

c^+ not precipitated in bubbles.

By introduction of (7) into (6) the resolution rate is given by

$$\Gamma = (\beta t - c^+)\frac{3}{2} \; \frac{RT \, d \cdot \eta}{b \, \sigma} \qquad (8)$$

Furthermore we need a treatment of the precipitation of gas at grain boundaries. If one assumes that atomic diffusion of the gas is the only transport mechanism, one obtains the following relation for the flux of gas toward grain boundaries

$$g = c \left[1 - \sum_{n=1}^{\infty} \frac{6}{\Pi^2 \, n^2} \exp\left(-n^2 \, \Pi^2 \, Dt/a^2\right) \right] \qquad (9)$$

where a is the radius of the grain, and D the temperature dependent diffusion coefficient. For the derivative follows

$$\dot{g} = \text{Pos}\ (\dot{c}) \left[1 - \sum_{n=1}^{\infty} \frac{6}{\Pi^2\, n^2} \exp\ (-n^2\ \Pi^2\ Dt/a^2) \right]$$

$$+ \frac{6c}{a^2} \sum_{n=1}^{\infty} \exp\ (-n^2\ \Pi^2\ Dt/a^2) \qquad (9a)$$

By using (5), (8) and (9a) one obtains the final expression

$$\dot{c} = \beta - \frac{Kc}{\sqrt{\beta}} (\beta t - c - g)^{\frac{1}{2}} + C_o\ (\beta t - c - g) - \dot{g}$$

$$\dot{g} = \text{Pos}\ (\dot{c}) \left[1 - \sum_{n=1}^{\infty} \frac{6}{\Pi^2\, n^2} \exp\ (-n^2\ \Pi^2\ Dt/a^2) \right] + \qquad (10)$$

$$+ \frac{6cD}{a^2} \sum_{n=1}^{\infty} \exp\ (-n^2\ \Pi^2\ Dt/a^2)$$

$$K = D\ \left(\frac{6\ \Pi\ n\ \beta\ R\ T}{\sigma}\right)^{\frac{1}{2}}$$

$$C_o = \frac{3}{2}\ \frac{R \cdot T \cdot d \cdot n}{b \cdot \sigma}$$

The system of equations (10) can be integrated numerically.

2.3 Insertion of the fission gas equation in a computer code system

a) A FORTRAN-code LANGZEIT has been developed providing numerical integration of equations (10) as a function of the irradiation time t. The fuel temperature which represents the most important rate controlling parameter has been inserted in the code as a separate subroutine. The spatial fission gas distribution in a fuel pin is calculated with a predetermined radial and axial temperature profile. The code permits the calculation of swelling, gas release ratio and gas in solution. In Fig.1,2, and 3 and in /9/ the concentration of the three quantities "c", "b" and "g" as a function of the irradiation time for a mixed oxide fuel burned up at a rating of 200 W/g can be seen. Fig. 4 presents the ratios of the three quantities. As one can see the trend of the gas is to rest in solution at low burn-up. In the following stage nearly all the gas is precipitated in bubbles and finally at high burn-ups the gas is released in sinks. The time dependence for these three phenomena is roughly an exponential function of the temperature.

b) During the rapid temperature increases, which occurs in power transients in a time range of some ten milliseconds, the concentration "c", "b" and "g" may be strongly affected. Therefore equations (10) have been suitably transformed in order to study the short-time behaviour. As mentioned before, the main parameter controlling the gas kinetic is the coefficient of diffusion. In order to perform the calculation with varying temperatures an analytical form for D has been assumed:

$$D = 0.25 \exp (100 \text{ kcal/mol} / RT) + D^{+}$$

where D^{+} is the radiation enhanced term. Equation (10) can be integrated for the case of a time dependent diffusion coefficient by taking the variable substitution

$$\tau = D \cdot t$$

With this substitution the equation (10) can be used in the transient routine KURZZEIT.

The only assumption made in the integration of (10) is that the gas within the bubbles is always in equilibrium with the surrounding matrix. The validity of such a hypothesis will be discussed later.

In order to check the validity of the input parameters of our code, several fuel samples have been analyzed by electron microscopy for a comparison with LANGZEIT /5/. In particular the calculated values of "c" have been compared with experimental measurements /8/. The agreement obtained is very good.

3. Fuel pin behaviour during rapid overheating transients

3.1 Physical processes involved

Let us suppose that a fuel had been irradiated for a certain time at a standard temperature regime. That means the temperature is slowly decreasing during each reactor cycle and repeates from cycle to cycle monotonic decays. During this time the fission gas is partly held in solution in interstitials or vacancies. The gas frozen in the lattice occupies little space and does not generate relevant swelling in the fuel. From Fig. 1 one can see that up to temperatures around $1500^{o}K$ the amount of gas in solution attains relevant values. In these cases the lattice is strongly oversaturated with gas. When the fuels (or fuel zones) are subjected to a temperature increase the gas atoms begin jumping into different lattice sites until, encountering other atoms of gas, they form stable complexes and finally bubbles. Depending on the temperature increase, this process can take some hours or fractions of seconds. The final result is in all cases the same, the fuel swells. In other words we can say that the lattice relaxes, in a short time, the atomic strains created during the entire irradiation period by the fission spike displacements by which the gas atoms have been re-ejected into solution. This energy, stored in these processes, is now converted into mechanical expansion of the fuel. This phenomenum arises from two distinct physical processes.

i) The first one is a mere precipitation of the gas. It is a thermally activated process with activation energies of the order of magnitude of some eV and therefore it can be hardly affected by the external stress field of the fuel.

ii) The other is the growth of the bubbles by capture of vacancies, in order to attain the equilibrium pressure with the solid. This process has a rate depending on the bubble size and "a priori" it could be retarded by the presence of external constraints. Practically applied stresses of the order of magnitude of 10^3 atm are required in the examined cases for hindering the bubble expansion.

We can thus conclude that transient swelling has to be considered as unrestrainable in a fuel with standard clad.

3.2 Application of the model to an LMFBR-type pin

For KURZZEIT a transient experiment made by Westinghouse in the TREAT-facility /6/, has been analyzed on the basis of the published data. In this experiment a fuel was burned to 1% at low temperature and then subjected to a in-pile power excursion. Fig. 5 shows the fuel structure before and after the transient. It is worth remarking that the intragranular bubbles after the transient have concentrations between 5-7 · 10^{14} cm^{-3}. That means the same order of magnitude as that observed under steady state conditions. These results are in agreement with our calculations for the bubble migration rates and coalescence frequency which predicts a bubble encountering probability of less than 2% at the highest transient temperatures.

KURZZEIT calculations have been performed taking the published distributions of temperature /6/. Fig. 6 shows the result of the calculations for the central part of the fuel and the periphery. It can be seen, that the fission gas swelling calculated is in good agreement with the values measured on the micrograph with the "Quantimet". It must be mentioned that the part of the swelling curves with negative slope represent the shrinkage of the bubbles following a temperature decrease. This process is probably not observed because it is slower than the expansion.

Furthermore, the behaviour of a pin in a power transient has been investigated. The steady state temperature has been assumed as $1350^{o}K$.

A power ramp initiated by 30 \$/sec has been taken as an example of an accident. The power and the temperature during the transient has been calculated with the REX-code /7/.

Fig. 7 shows the trend of "c", "b" and "g" during the transient. One can see, that the effect of the temperature increase is that of transferring the gas from the phase "c" into "b", without affecting the concentration "g". Eventual gas release phenomena connected with power transient have, therefore, to be ascribed to formation of cracks through closed macro porosity, in which part of the gas "g" is retained.

Fig. 8 shows the swelling ratio during the excursion time for pins previously irradiated at 150 W/g for different burn-ups.

From the curves of Fig. 8 we can deduce the following remarks:

i) The transient swelling attains critical values for the stability of the clad, even at 2% burn-up. The swelling is rapidly increasing with the burn-up previously attained by the fuel. For higher burn-ups (greater than 5%) we expect clad rupture before the gas precipitation process goes to completion.

ii) At temperatures around 2000^{o}K the swelling of the fuel takes place immediately (in the order of 10 msec). Therefore excursions above this threshold, even limited to short times, lead to clad rupture at burn-ups above 2-3%.

4. Calculation of the swelling strains in LMFBR type cores during unprotected overpower transients

The concentrations "c", "b" and "g" obtained with LANGZEIT were first used as the initial conditions for a hypothetical disassembly analysis performed with KADIS /3/. The concentrations were calculated with a radial and axial core power shape function. A more sophisticated treatment however, would include a 2-dimensional temperature profile in the fuel pins. Furthermore it would be more justified to integrate the subroutine KURZZEIT in the disassembly code. Nevertheless substantial information can be obtained by the results achieved with our KURZZEIT calculations for a hypothetical accident.

As an example, we have assumed two different fast reactor cores. The first is a very asymmetric cylindrical core (SEFOR type) with a steady state power of 730 MW thermal. This special example has been chosen in order to study a possible influence of the strongly asymmetric power shape. The second one is a core of the SNR-300 reactor type. For the calculations the core was devided into 5 axial regions (Z). In the radial direction (R) 5 zones were assumed for the first example and 2 for the SNR-300 type. Additionally, each pin cross section (which is specified by two coordinates, Z and R), has been divided into 5 radial (r) zones where the local temperature of the fuel is accounted for.

In each cell the history of the fission gas in the fuel has been previously calculated with LANGZEIT. The accidents under investigation were defined as reactivity transients calculated with the REX-code. This provided the input temperatures and the fission rate for the KURZZEIT subroutine.

A continuous description of the gas kinetics and the values of the engendered swelling were obtained as a function of the accident time.

4.1 SEFOR type core

Fig. 9 shows the maximal average temperature of the different fuel elements after 200 msec. The excursion was initiated with a ramp rate of 30 $/sec. In Fig. 10 the pin swelling ratios, at the same time are plotted versus radial and axial coordinates.

The average burn-up of the fuel was 4%. The shadowed part of the surface corresponds to values of swelling above 2% which is a probable limit for clad cracking. It can be seen, that a large number of pins should burst. Fig. 11 shows the same effect when the average burn-up is doubled. In this case nearly all the pins should fail, the central ones being practically destroyed within the first milliseconds of the accident.

4.2 SNR-300 type core

A similar accident was calculated for the SNR-300 type reactor core. The maximal temperatures reached during the overpower transient are plotted in Fig.12, for 5 axial cross sections. The swelling profiles are shown for three different transient times. The pin under investigation was assumed to be previously burned-up at an average power of 150 W/g.

4.3 Discussion

By studying the behaviour of the fission gas during these transients one can argue that the swelling is mainly controlled by the precipitation kinetics of the gas "c" in solution. This process depends both on the concentration of "c" at the beginning of the accident and on the local temperature increase during the transient. Fig. 13 shows the decay of "c" in different radial fuel-zones of a SNR-300 fuel pin. The section is located in the inner zone of the core and in the upper third of the axial height. "c" decreases during a time period of 100 msec by about one order of magnitude in the center of the pin. At the periphery of the pin the concentration remains nearly constant, because the gas mobility increase during the transient is not large enough to permit migration of gas atoms to the bubbles+). In the intermediate regions the amount of gas precipitated depends on the elapsed transient time.

+) In order to precipitate into the next bubble the gas atoms have to migrate a distance < d > of about 500 Å. This migration time and the fuel temperature are related by the following equation.

$$t_m = \frac{\langle d \rangle^2}{6D_o} \exp\left(\frac{\Delta H}{RT}\right)$$

where ΔH is the migration enthalpy.

The fuel zones which attain in the early stage of the transient (less than 50 msec) temperatures of more than $2000^{o}K$, contain usually at the beginning of the accident negligible amount of gas in solution. In these zones a minor swelling is produced by a pressure build-up in the pre-existent bubbles.

In the central regions of those pins, where the melting temperature is reached during the transient under investigation, the swelling can produce material extrusion along the central channel. This eventuality was not taken in to account in our calculations, which have been performed only for cases where no substantial melting occurs.

From the axial swelling patterns it is possible to predict the positions where failures are expected to occur during the transient. If one assumes that at the beginning of the transient there is no gap between fuel and clad, 2 factors determine the position of the failure

1) The local expansion of the fuel during the transient.

2) The previous restrains caused by steady state swelling.

As shown in Fig. 14 the maxima of "steady state" swelling are attained in the middle of the pin length. But during the transient the largest expansions are produced between the middle and the bottom of the pin. This depends on the larger concentration of dissolved gas in the cold axial cross sections. Since the temperature increase is here relatively lower, more time is needed for precipitation. As a consequence the maximum of the transient swelling is displaced to lower positions with the time, as long as the clad can resist the produced strains[+)].

+) Since the transient swelling patterns are extremely dependent on the power shape function, these results cannot be generalized.

In Fig. 14 the regions of a pin, expected to burst, are indicated for different "survival times".

5. Conclusions

The results calculated in KURZZEIT can be used in a disassembly code as VENUS-II for the analysis of a hypothetical accident. To get a better knowledge of the role of the rare gases in an overpower accident however, it seems to be necessary to use more sophisticated code systems such as SAS3A-VENUS-II. But as a first evaluation, one can draw the conclusion, that the large swelling we calculated with our model will result in a very early pin failure. This will lead to early disassembly and therefore the reactor will be shut down earlier. As a logical consequence the integrated energy and therefore the mass of molten fuel are substantially reduced.

References

/1/ G. Heusener, G. Kessler

Kernforschungszentrum Karlsruhe, KFK-1834 (1973)

/2/ W.R. Bohl et al.

Analysis of Hypothetical Accidents for SNR-300

Conference of Engineering of Fast Reactors for Safe and Reliable Operation, p. 1235, Karlsruhe, Oct. 1972

/3/ H.G. Bogensberger, E.A. Fischer and P. Schmuck

On the Equation of State of Mixed Oxide Fuel for the Analysis of Fast Reactor Disassembly Accidents

Conference on Fast Reactor Safety, Beverly Hills, California, April 1974

/4/ C. Ronchi and H.J. Matzke

Calculations on the In-Pile Behaviour of Fission Gas in Oxide Fuels

Journal of Nuclear Materials Vol. 45 (1972/73) p. 15-28

/5/ C. Ronchi, H.J. Matzke

Fuel and Fuel Elements for Fast Reactors

International Atomic Energy Agency, Vienna (1974) p. 57

/6/ G. Culley et al.

Response of an EBR II irradiated mixed oxide fuel pin to an overpower transient in treat

ANS Meeting on Fast Reactor Fuel Element Technology New Orleans, 1971

/7/ K. Hornyik

Kernforschungszentrum Karlsruhe, KFK-799 (1968)

/8/ H. Zimmermann

Spaltgasverhalten in Oxidbrennstoffstäben für Schnelle Brüter

Reaktortagung Berlin 1974, Tagungsbericht S. 372

/9/ H.G. Bogensberger and C. Ronchi

Ein Programmsystem zur Berechnung des Einflusses der Spaltgaskonzentration bei Transienten in schnellen Reaktoren

Reaktortagung Berlin 1974, Tagungsbericht S. 110

/10/ R.S. Nelson

J. Nucl. Vol. 31, 153 (1969)

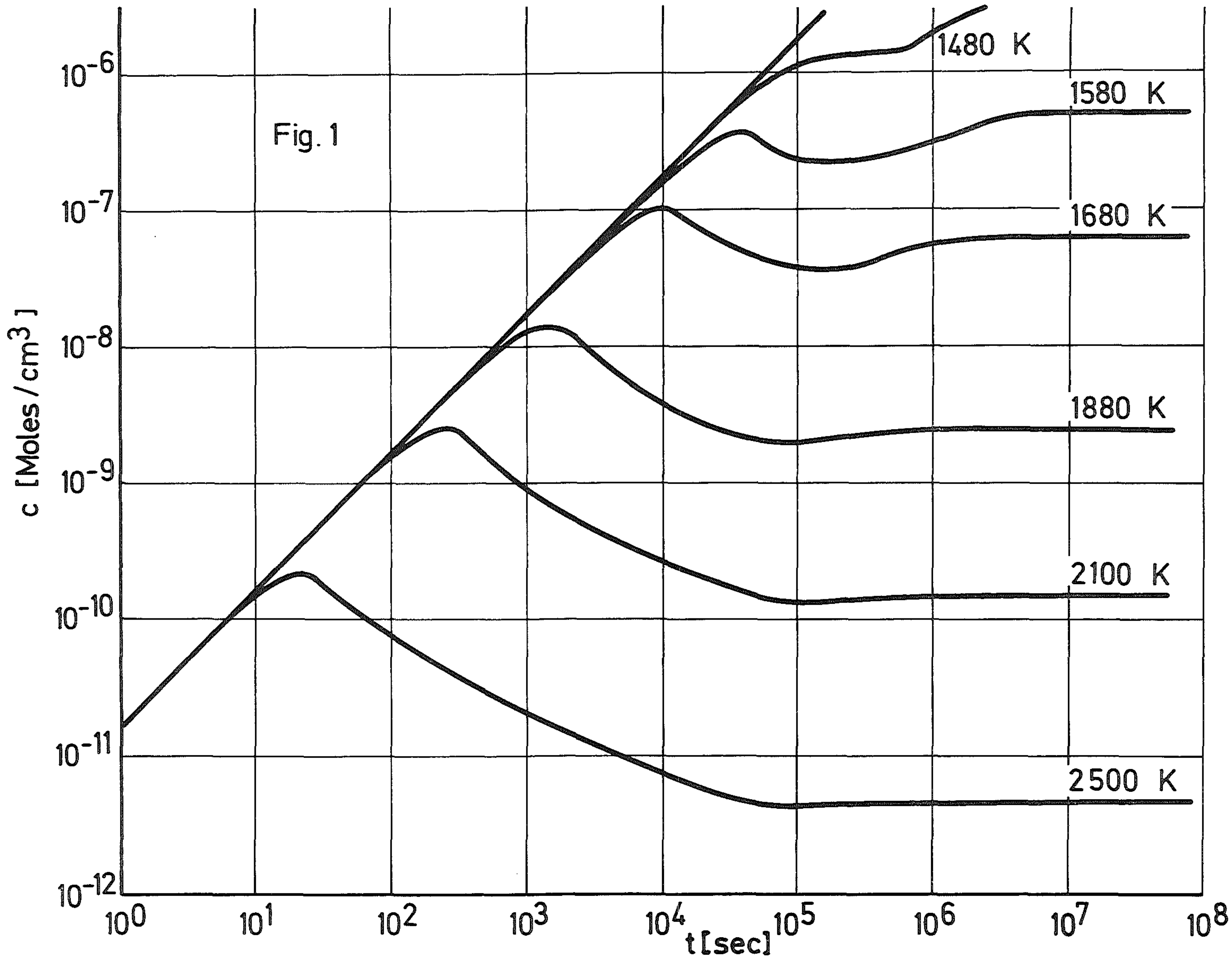
c [Moles / cm³]
10⁻⁶
10⁻⁷
10⁻⁸
10⁻⁹
10⁻¹⁰
10⁻¹¹
10⁻¹²
10⁰
10¹
10²
10³
10⁴
10⁵
10⁶
10⁷
10⁸
t [sec]
1480 K
1580 K
1680 K
1880 K
2100 K
2500 K

Fig. 1

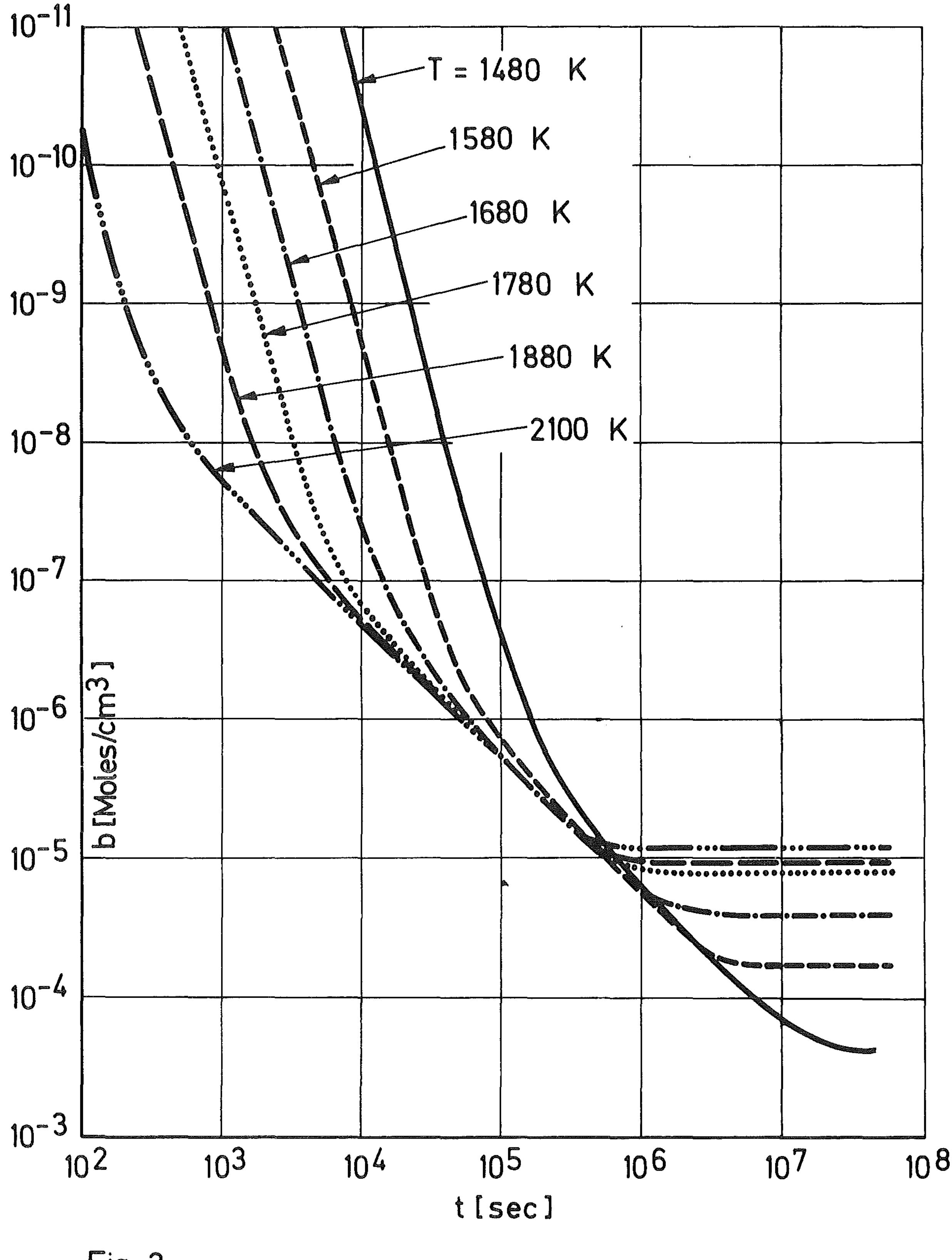
T = 1480 K
1580 K
1680 K
1780 K
1880 K
2100 K
10^{-11}
10^{-10}
10^{-9}
10^{-8}
10^{-7}
10^{-6}
10^{-5}
10^{-4}
10^{-3}
b [Moles/cm^3]
10^2
10^3
10^4
10^5
10^6
10^7
10^8
t [sec]

Fig. 2

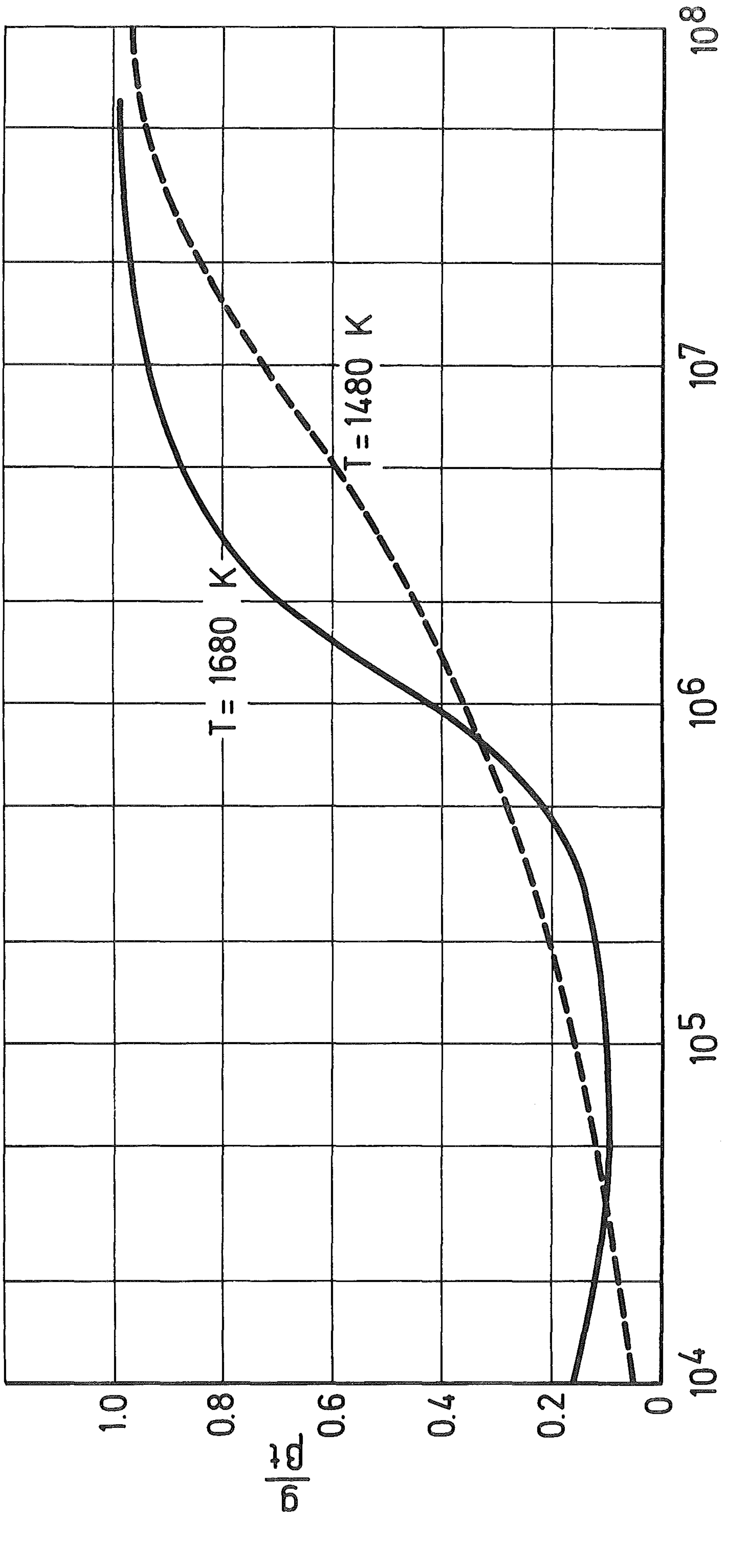

1.0
0.8
0.6
0.4
0.2
0
$\frac{b}{\beta_t}$
10^4
10^5
10^6
10^7
10^8
t [sec]
T = 1680 K
T = 1480 K

Fig. 3

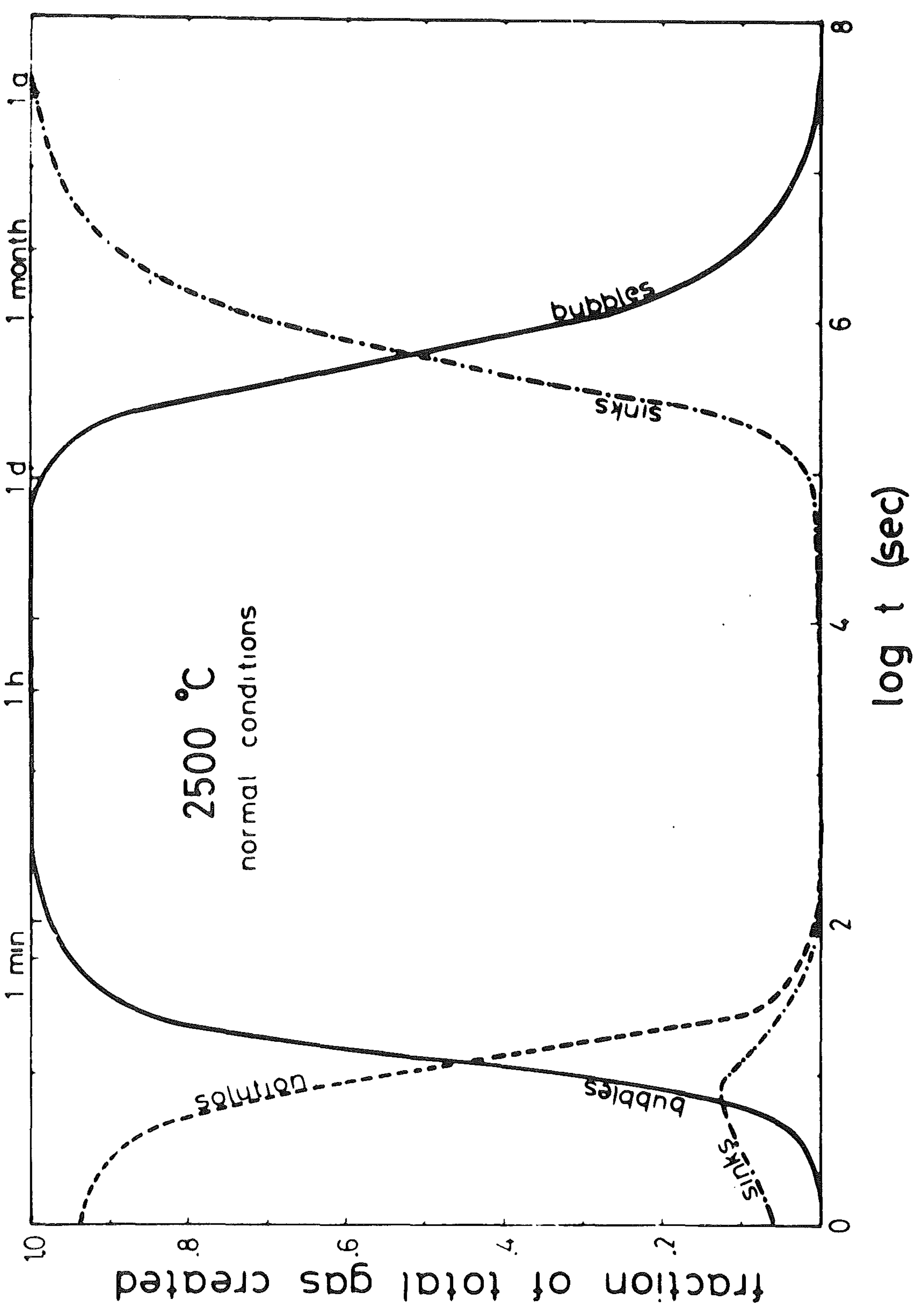
2500 °C
normal conditions
bubbles
sinks
solution
1 min
1 h
1 d
1 month
1 a
0
2
4
6
8
1.0
.8
.6
.4
.2
log t (sec)
fraction of total gas created

Fig. 4

$$\frac{\Delta V}{V} = 3 \sim 4\%$$

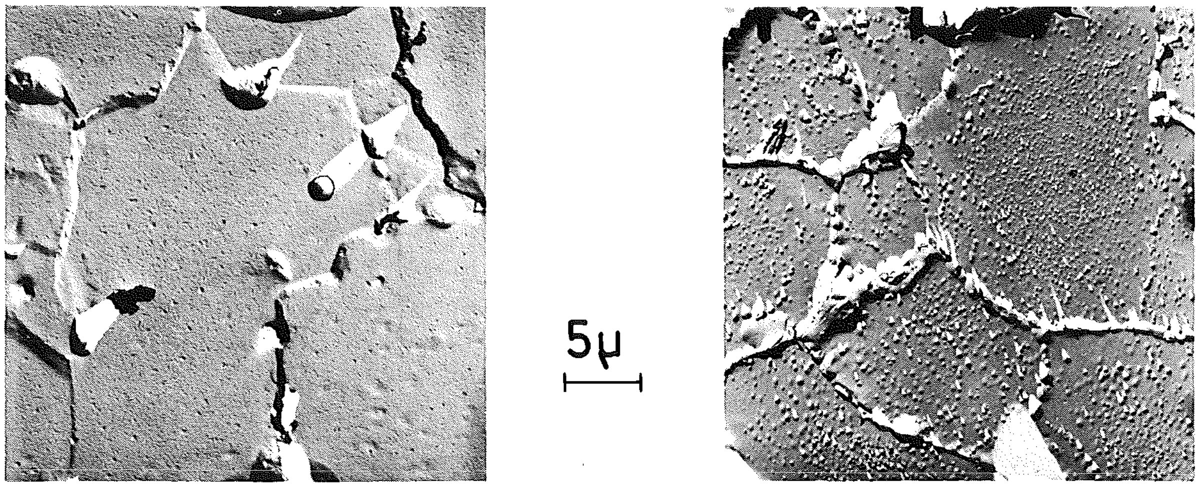

irradiated to 1% burn-up before the transient

the same sample after the transient

(REM micrographs)

Fig. 5

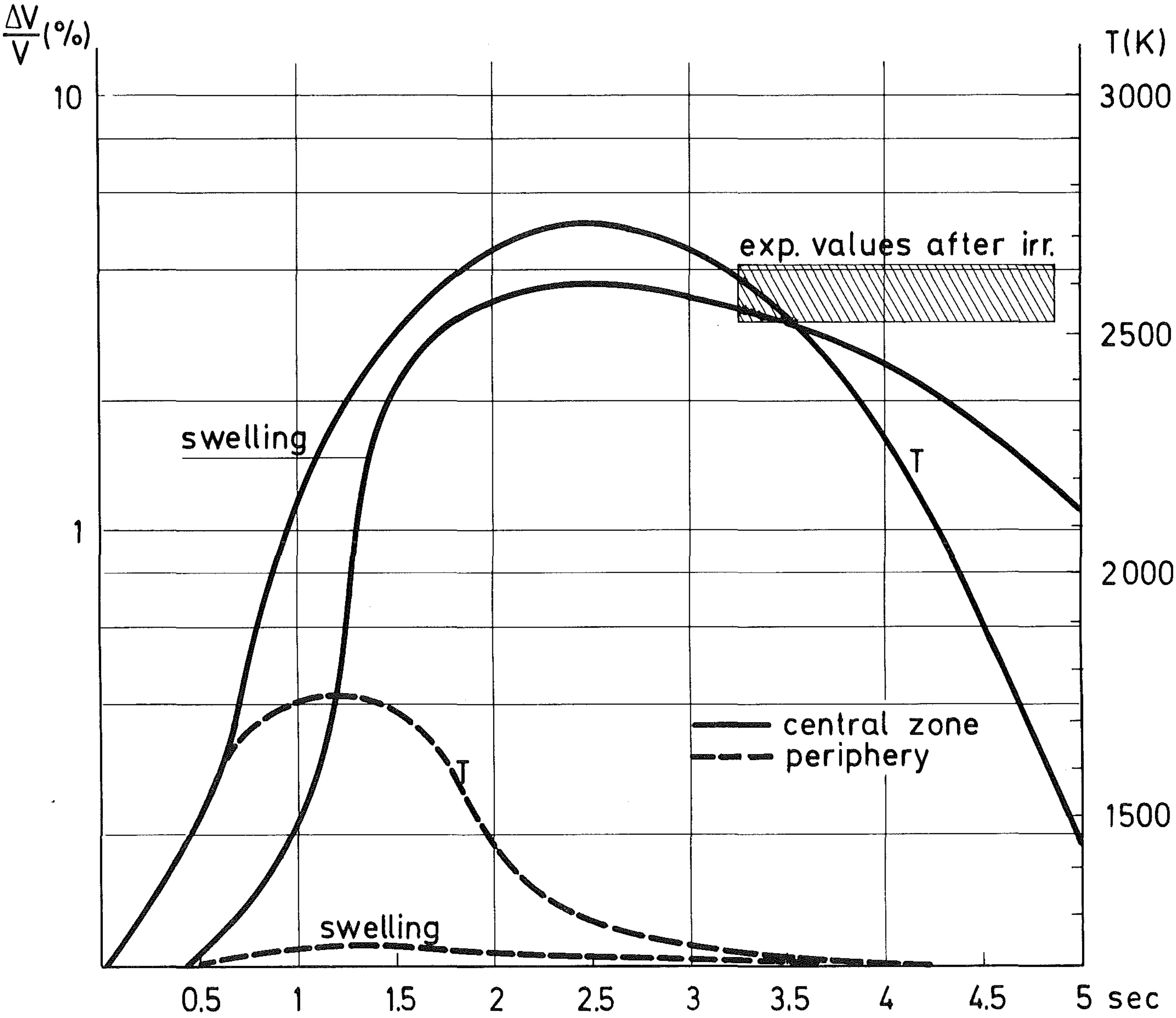

Fig. 6

Calculated and measured swelling of a pin after a controlled overpower transient.

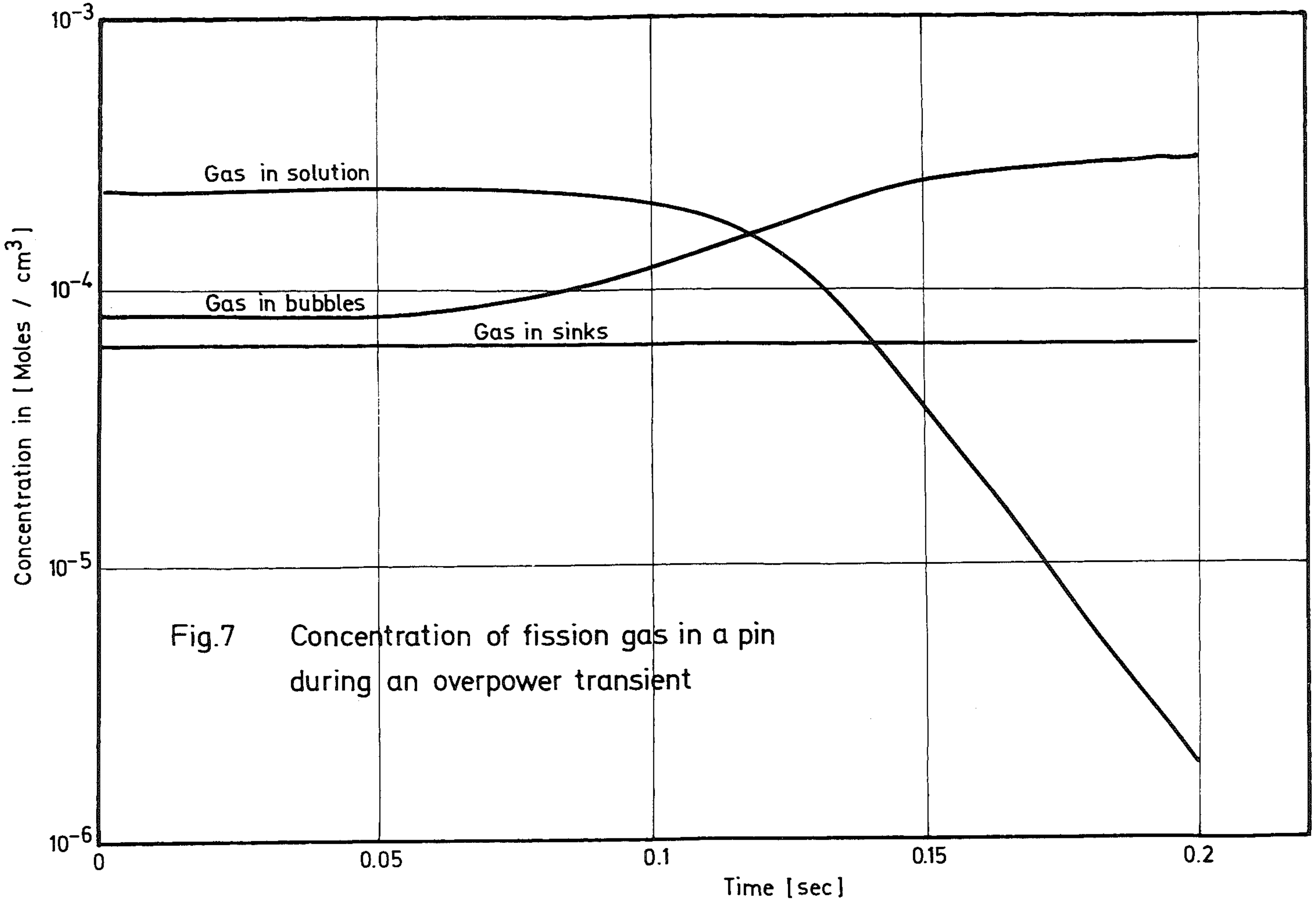

Fig.7 Concentration of fission gas in a pin during an overpower transient

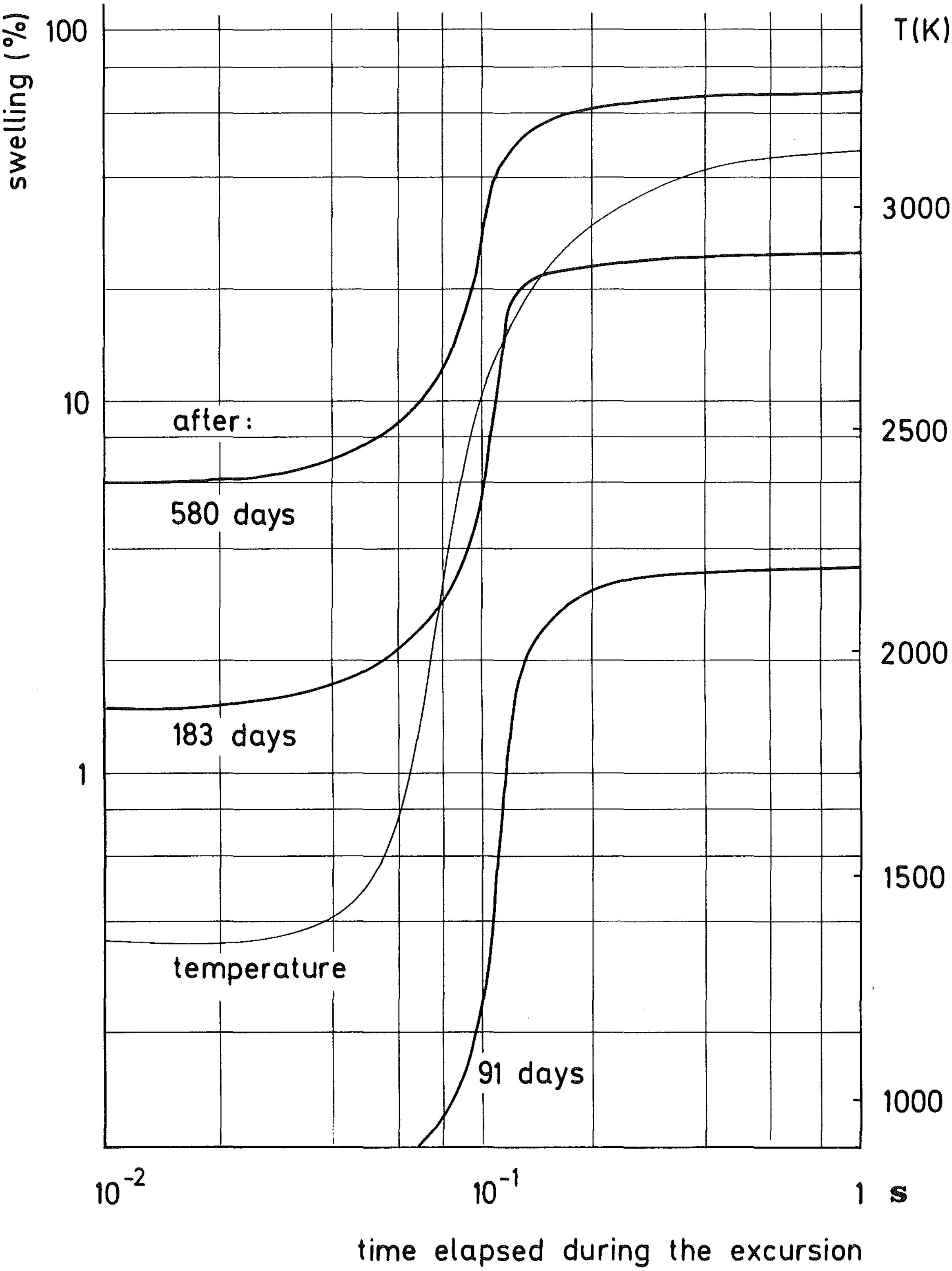
swelling (%)
100
10
1
T(K)
3000
2500
2000
1500
1000
after:
580 days
183 days
temperature
91 days
10^{-2}
10^{-1}
1 s
time elapsed during the excursion

Fig. 8

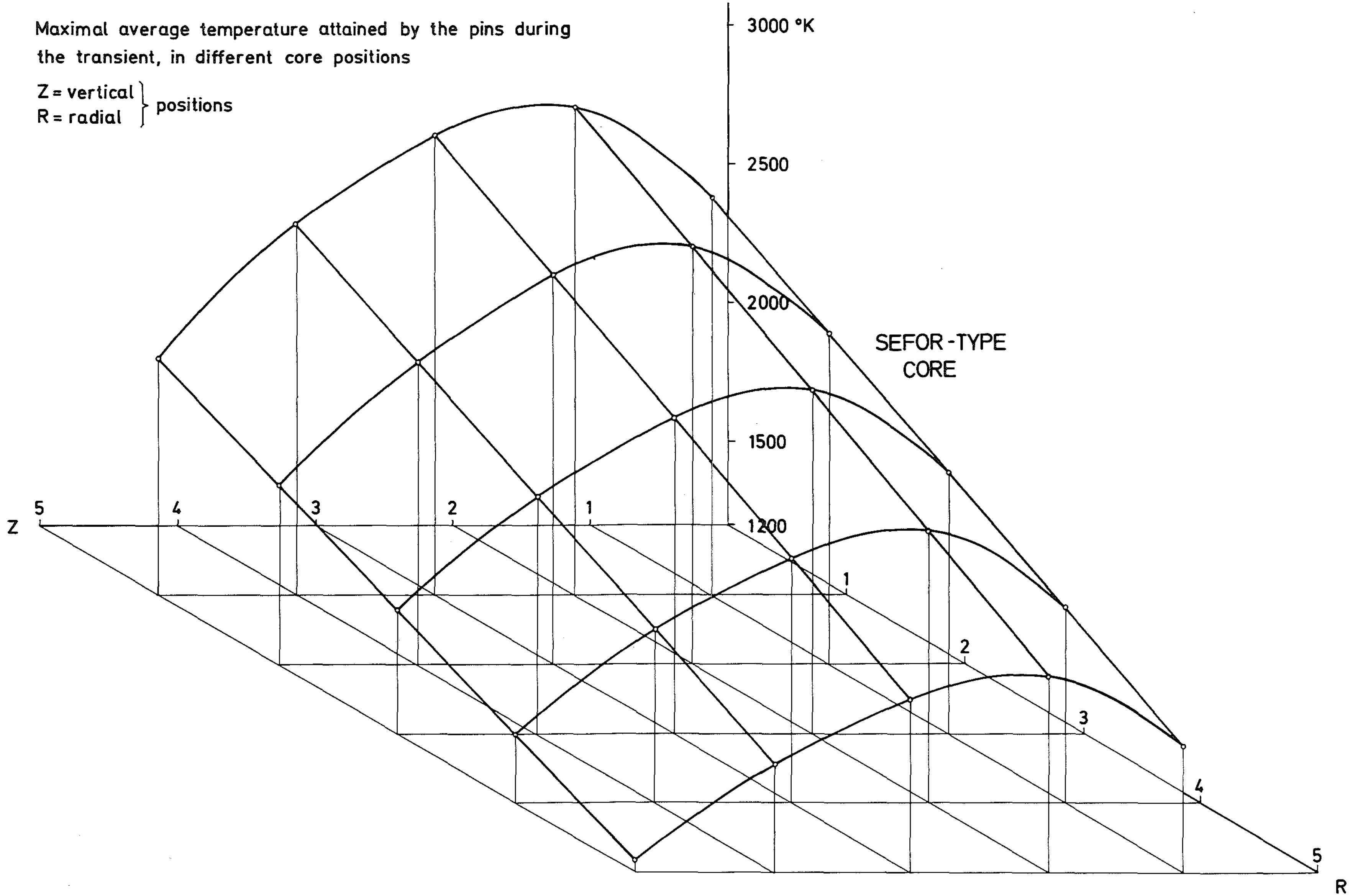
Maximal average temperature attained by the pins during
the transient, in different core positions
Z = vertical
R = radial
positions
3000 °K
2500
2000
1500
1200
SEFOR-TYPE
CORE
Z
5
4
3
2
1
1
2
3
4
5
R

Fig.9

F.G. Swelling in reactor core after 200 ms
from the beginning of the transient
ϱ max = 3 dollars

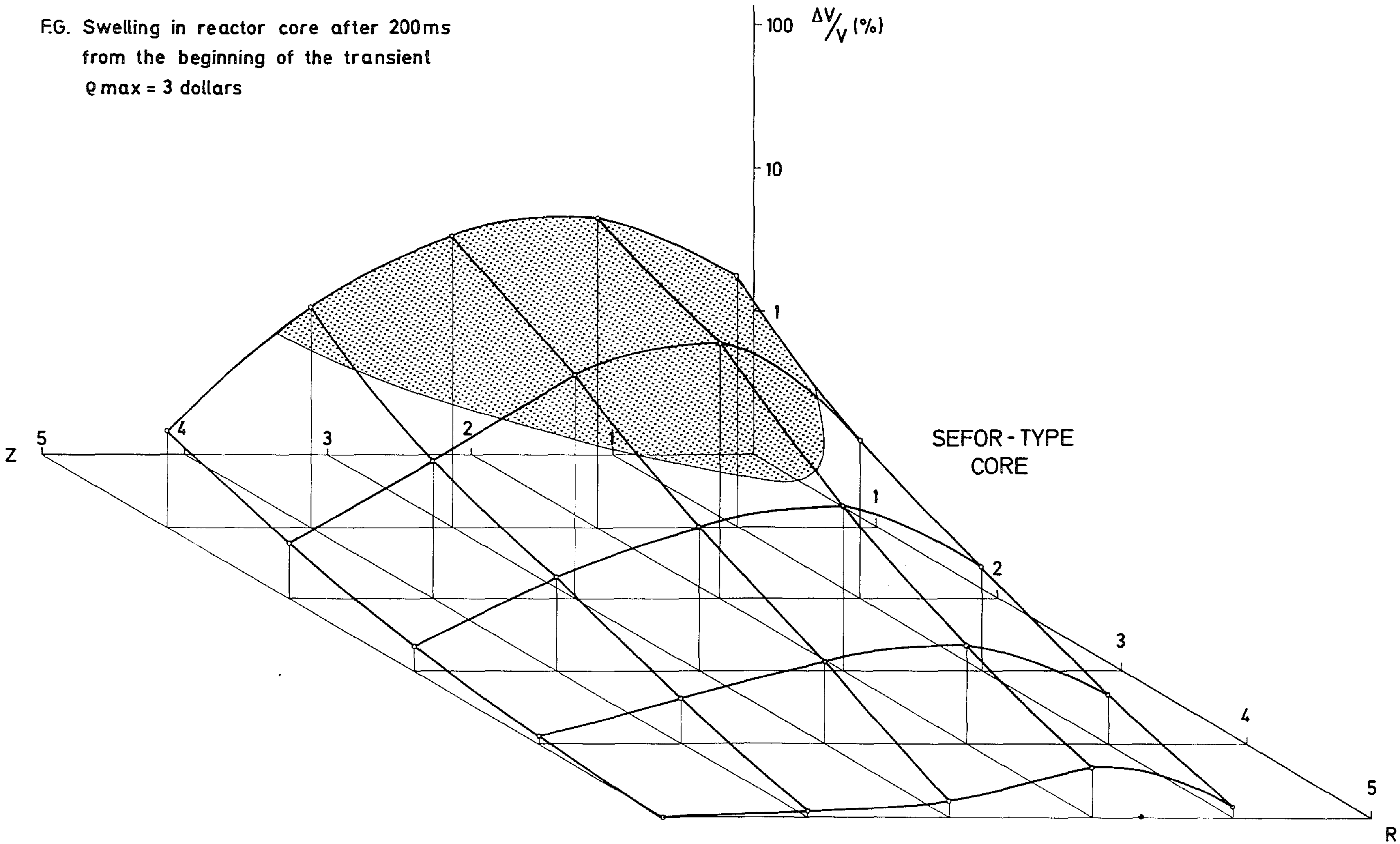

Fig. 10

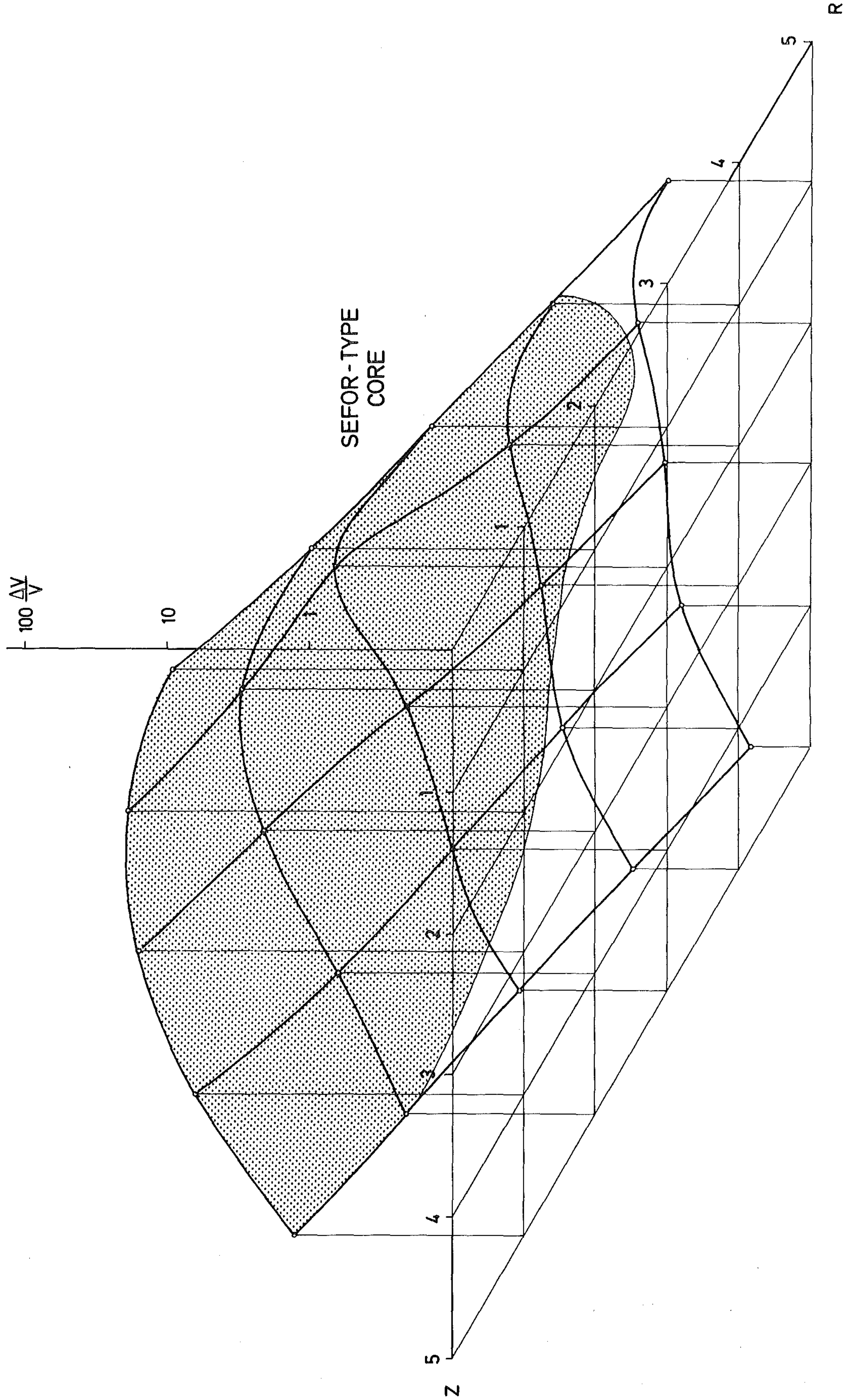

Fig.11

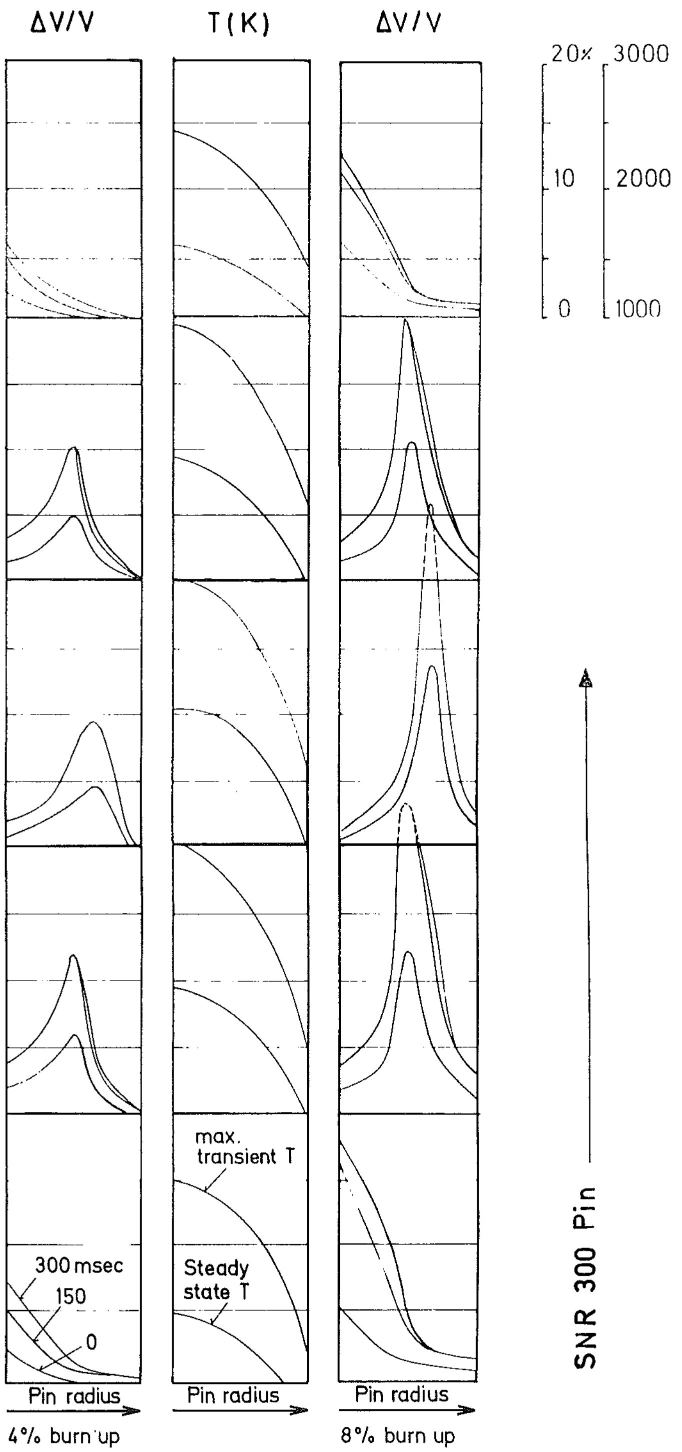

Fig. 12

Radial swelling profile (right and left) in 5 axial cross sections of an SNR-type pin during a rapid reactivity ramp. The curves in the zells represent the swelling at the beginning of the transient, 150 msec and 300 msec later, respectively.

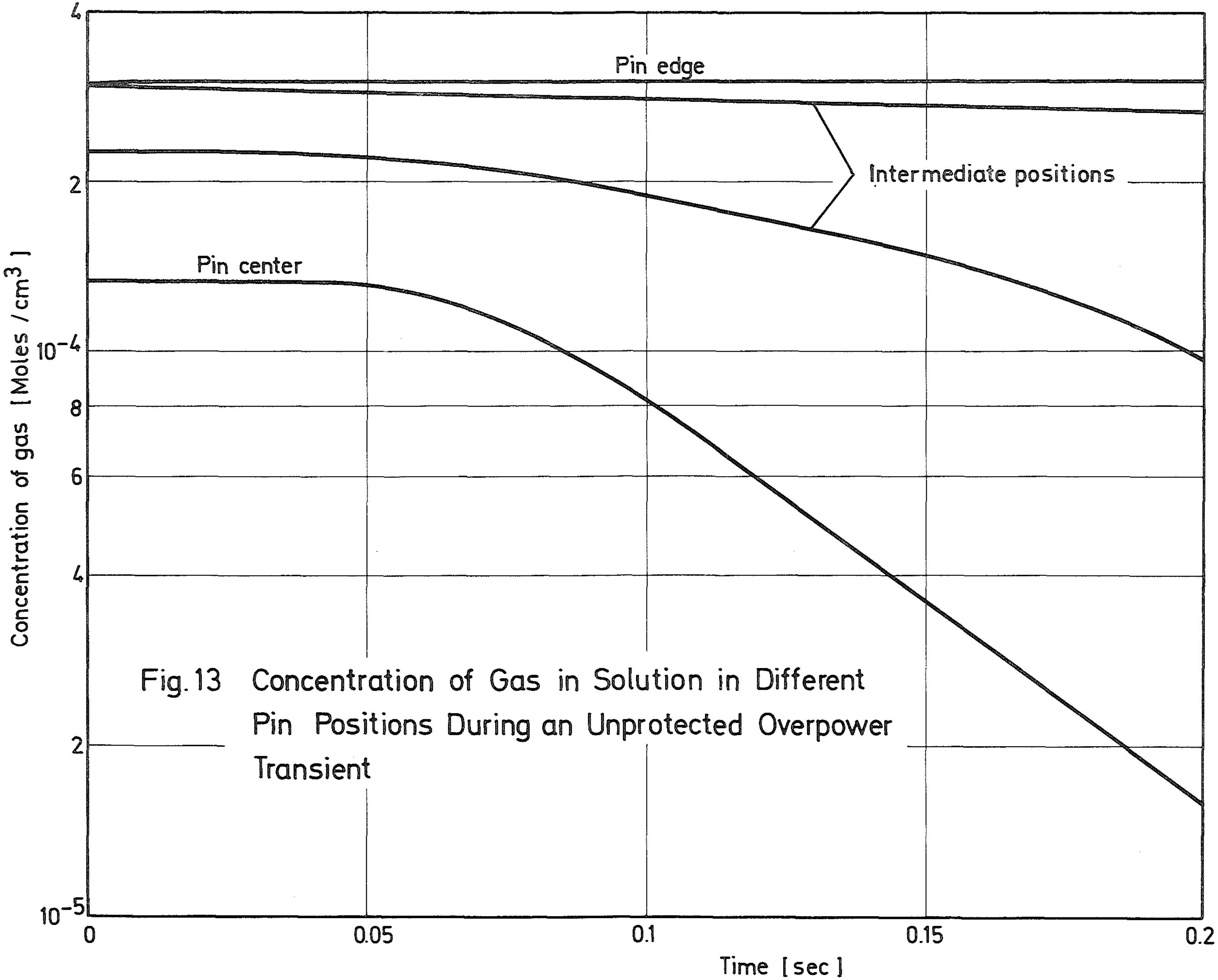

Fig. 13 Concentration of Gas in Solution in Different Pin Positions During an Unprotected Overpower Transient

0.0 s	0.05 s	0.1 s	0.2 s	0.3 s	time
0.3%	+0.2%	+0.3%	+0.3%	+0.3%	
1.9%	+1.5%	+1.8%	+1.8%	+1.8%	
2.5%	+2.3%	+2.4%	+2.4%	+2.4%	
2.1%	+2.0%	+2.5%	+2.6%	+2.7%	
0.3%	+0.3%	+0.5%	+0.7%	+1.4%	

4% burn-up

Swelling pattern of an SNR-type
pin during an overpower transient

0.0 s	0.05 s	0.1 s	0.2 s	0.3 s
1.1%	+0.9%	+1.1%	+1.3%	+1.4%
4.3%	+3.6%	+4.2%	+4.4%	+5.2%
5.6%	+5.4%	+5.4%	+5.4%	+6.4%
4.9%	+4.7%	+6.1%	+6.1%	+7.1%
1.3%	+1.4%	+1.9%	+2.5%	+2.8%

8% burn-up

Fig. 14